© 2021. Published by The Company of Biologists Ltd | Journal of Experimental Biology (2021) 224, jeb242386. doi:10.1242/jeb.242386

RESEARCH ARTICLE

The influence of the post-pulmonary septum and submersion on the pulmonary mechanics of *Trachemys scripta* (Cryptodira: Emydidae)

Ray Brasil Bueno de Souza and Wilfried Klein*

ABSTRACT

The respiratory system of chelonians needs to function within a mostly solid carapace, with ventilation depending on movements of the flanks. When submerged, inspiration has to work against hydrostatic pressure. We examined breathing mechanics in *Trachemys scripta* while underwater. Additionally, as the respiratory system of *T. scripta* possesses a well-developed post-pulmonary septum (PPS), we investigated its role by analyzing the breathing mechanics of lungs with and without their PPS attached. Static compliance was significantly increased in submerged animals and in animals with and without their PPS, while removal of the PPS did not result in a significantly different static compliance. Dynamic compliance was significantly affected by changes in volume and frequency in every treatment, with submergence significantly decreasing dynamic compliance. The presence of the PPS significantly increased dynamic compliance. Submersion did not significantly alter work per ventilation, but caused minute work of breathing to be much greater at any frequency and ventilation level analyzed. Lungs with or without their PPS did not show significantly different work per ventilation when compared with the intact animal. Our results demonstrate that submersion results in significantly altered breathing mechanics, increasing minute work of breathing greatly. The PPS was shown to maintain a constant volume within the animal's body cavity, wherein the lungs can be ventilated more easily, highlighting the importance of this coelomic subdivision in the chelonian body cavity.

KEY WORDS: Breathing mechanics, Compliance, Work of breathing, Respiratory system, Testudines, Reptilia

INTRODUCTION

Pulmonary compliance is a measure of the distensibility of the lungs and can be obtained by determining the relationship between changes in lung volume and intrapulmonary pressure (Klein et al., 2003). Pulmonary compliance can either be analyzed from a static perspective (C_{stat}), providing information about the work needed to overcome the elastic forces of a system in resting conditions (Jackson, 1971), or from a dynamic situation (C_{dyn}), by combining different respiratory frequencies (f_R) and tidal volumes (V_T) to evaluate the active character of the ventilatory mechanics (Vitalis and Milsom, 1986a). The muscles related to the respiratory system must produce enough strength to overcome the resistance associated with the expansion of the lungs and body wall (Reichert et al., 2019) so that the total compliance of the respiratory system (C_T) is composed of the compliance of the lungs (C_L) and the compliance of the body wall (C_B).

In general, reptilian lungs are quite compliant, with the body wall being the major component of elastic resistance to airflow (Vitalis and Milsom, 1986a), while the alveolar lungs of mammals are much less compliant and generate the main resistance itself (Crosfill and Widdicombe, 1961). Differently from mammals, reptiles show a great diversity in their lung morphology, which can vary in the number of internal chambers, and in the type and distribution of the parenchyma in the organ (Perry, 1998). Although still poorly investigated, studies that analyze the ventilatory mechanics of reptiles have revealed that the compliance of reptilian lungs can be influenced by their degree of compartmentalization and parenchymal type (Reichert et al., 2019; Vitalis and Milsom, 1986a).

Testudines possess multicameral lungs and a more rigid body wall because of the presence of a shell, which leads to a smaller body wall compliance (Vitalis and Milsom, 1986a). Additionally, unlike any other amniotes, they do not use their intercostal muscles for ventilatory movements, as their ribs are fused to the shell; instead, they depend on muscles not normally associated with this function to move the entire visceral cavity to generate changes in pulmonary volume and pressure. Submerged semiaquatic turtles sitting in shallow water may only extend their neck to penetrate the water's surface with their nostrils, minimally disturbing the water while episodically breathing air. Under such circumstances, the flexible body wall will be several centimeters below water, and so exposed to hydrostatic pressure. In such situations, exhalation may be passive as a result of the hydrostatic pressure compressing the abdominal cavity and reducing lung volume, while inhalation may be passive when the same animals are out of the water, as a result of gravity pulling the viscera away from the lungs, increasing their volume (Gaunt and Gans, 1969). While exhalation might be passive in submerged turtles, inhalation will be an active process, needing more muscle contraction to expand the body cavity against the surrounding hydrostatic pressure. Following this idea, one objective of the present study was to investigate the effects of submergence on the ventilatory mechanics of semiaquatic turtle *Trachemys scripta* (Thunberg in Schoepff 1972), asking to what extent the mechanical cost of breathing will increase in submerged animals.

The lungs of testudines show mainly heterogeneously distributed parenchyma concentrated in the central and dorsal region (Perry and Duncker, 1980), in addition to being dorsally attached to the carapace and covered ventrally by a post-pulmonary septum (PPS), isolating the lungs from the other viscera (Perry and Duncker, 1978;

Departamento de Biologia, Faculdade de Filosofia, Ciências e Letras de Ribeirão Preto, Universidade de São Paulo, 14040-901 Ribeirão Preto, São Paulo, Brazil.

*Author for correspondence (wklein@usp.br)

R.B.B.d.S., 0000-0001-5388-5402; W.K., 0000-0001-6099-6178

Received 4 February 2021; Accepted 28 May 2021

Journal of Experimental Biology (2021) 224, jeb242386. doi:10.1242/jeb.242386

Perry and Sander, 2004). The PPS is further connected to the liver directly through a ventral mesopneumonium as well as indirectly through the stomach and the ventral mesentery, while laterally the PPS is connected to the carapace (Lyson et al., 2014). Among testudines, the degree of development of the PPS varies, so that in highly active marine species the PPS is well developed, while in some aquatic species with sedentary habitats it is reduced, even being absent in some species (Lambertz et al., 2010; Perry, 1998; Perry and Sander, 2004). *Trachemys scripta* presents a very muscular PPS (von Hansemann, 1915; Perry, 1983; Perry and Sander, 2004) that covers the ventral part of the lungs and is laterally fixed to the carapace, with the exception of the caudal lung regions, which extend freely into the remaining body cavity (see Fig. S1; Lambertz et al., 2010). These characteristics cause the cranial and central regions of each lung to be kept more immobile, while the posterior regions carry out the main volume changes (Perry and Duncker, 1978). The influence of the PPS on breathing mechanics in turtles, however, has not yet been investigated experimentally; in the present study, we analyzed the effect of the PPS on *T. scripta* lungs that still have the PPS connecting the lungs and body wall, compared with lungs that are free from the PPS. Such a comparison could highlight the importance of a functional separation of the lungs from the remaining viscera, even if it is an incomplete separation as seen in *T. scripta*, as highly efficient respiratory systems, such as those seen in birds and mammals, have evolved such a complete separation (Klein and Owerkowicz, 2006).

MATERIALS AND METHODS

Animals

Ten juvenile red-eared slider turtles (*Trachemys scripta*, 230±80 g) of both sexes were obtained from the Jacarezário, Universidade Estadual Paulista – Campus Rio Claro, transported to the animal care facility of the Biology Department of the Faculdade de Filosofia, Ciências e Letras de Ribeirão Preto (FFCLRP), and maintained there for up to 1 month before experimentation in polypropylene boxes with both wet and dry regions, under a 12 h light/dark cycle at 25±2°C. The experimental protocol was approved by the ethics committee of the FFCLRP, protocol number 2020.1.267.59.9, and animals were used under federal approval (SISBIO number 35221-10).

Experimental protocol

Animals were killed by an intraperitoneal injection of thiopental (150 mg kg^{-1}) and lidocaine (5 mg kg^{-1}), to avoid pain and discomfort during application. This dosage of thiopental caused analgesia and led to interruption of respiratory capacity within 20–30 min of application (Klein et al., 2003). The trachea was then immediately cannulated through a catheter connected to a three-way stopcock. For measurement of lung volume and static mechanics, one connection of the three-way stopcock led to a plastic syringe and another was connected to a water-filled tube leading to a pressure transducer (Deltran). The signal from the transducer was amplified by a signal amplifier (AECAD 04P) and registered within a data acquisition system (PowerLab 8/35) linked to LabChart 7.0 software (ADInstruments). In the intact animals, we started from the resting position of the respiratory system, where the lungs were fully expanded and allowed to return to their resting position. Next, known volumes of air were introduced in a stepwise manner into the respiratory system until a pressure of about +30 cmH_2O was reached, then the air was withdrawn stepwise to a pressure of −10 cmH_2O, and air was again injected stepwise until the initial lung volume was reached. The accompanying pressure changes were recorded to obtain static pressure–volume curves. Static volume curves were constructed 3 times, maximally inflating the respiratory system between each trial, and allowing the system to return to its resting position.

Table 1. Body mass (M_b), maximum lung volume (V_L) and resting lung volume (V_{Lr}) of animals used in the present study

M_b (kg)	V_L (ml)	V_{Lr} (ml)
0.070	4	1
0.173	22	2
0.194	30	10
0.198	26	6
0.210	12	3
0.239	42	12
0.265	52	17
0.288	48	8
0.296	45	5
0.332	50	10

For measurement of dynamic compliance and total work of breathing, the same apparatus was used, with the difference that in this case the tube leading to the syringe was connected in series to a pneumotachograph and then to an artificial respirator (Inspira, Harvard Apparatus). The changes in flow in the pneumotachograph were registered by a spirometer (FE141), whose signal was also fed into the data acquisition system and software. The spirometer was calibrated by applying a constant flow of 5 ml s^{-1} to the pneumotachograph. Predefined volumes of air (1, 2, 4, 6 and 8 ml) were injected into the respiratory system and then withdrawn by the ventilator at different frequencies (5, 10, 20, 30, 40 and 50 min^{-1}), thereby simultaneously measuring flow and pressure changes. Because of the factory settings of the mechanical ventilator used, ventilation was continuous with no pause between inflation and deflation, resulting in variable durations of inflation and deflation (0.6–6.0 s), and flow rates (0.2–13.3 ml s^{-1}), according to the combination of volume and frequency applied. The greatest flow rates resulted in a measurable resistance of the system, as a result of the small caliber of the intratracheal cannula (0.85 mm inner diameter, 14 mm length) used. To compensate for this, we ran every combination of volume and frequency without any animal attached to the intratracheal cannula, calculated resistive work for every

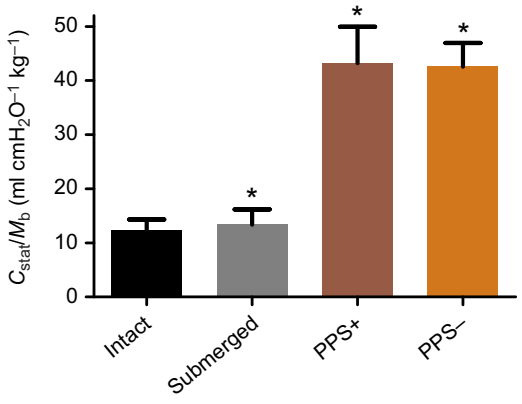

Fig. 1. Mean (±s.e.m.) static compliance (C_{stat}) for each treatment. Treatments groups were: Intact, animals out of water; Submerged, animals in a water bath; PPS+, exposed lungs with post-pulmonary septum (PPS) attached; PPS−, exposed lungs with PPS removed. For details, see Materials and Methods. Asterisks indicate a significant difference from Intact animals. M_b, body mass.

Journal of Experimental Biology (2021) 224, jeb242386. doi:10.1242/jeb.242386

combination and subtracted this value from the work values obtained at the corresponding combinations of volume and frequency applied to the animals.

The protocol was applied in the following sequence. (1) 'Intact' animals in a supine position on a table (static compliance N=10, dynamic compliance and work of breathing N=7). The supine position was chosen, as previous studies used the same position to analyze the static and dynamic breathing mechanics of reptiles (Perry and Duncker, 1978; Milsom and Vitalis, 1984; Vitalis and Milsom, 1986a), allowing us to compare our data with those given in the literature. (2) 'Submerged' animals in a prone position placed inside a water bath, covered with a column of approximately 5 cm of water above their carapace, extending the neck for the nostrils to break the water surface (static compliance N=8, dynamic compliance and work of breathing N=7). (3) Animals that had had their plastron removed, as well as all their limbs and organs, except for the lungs, which retained an intact PPS ('PPS+'; N=7). (4) Dissected animals that had had their PPS removed ('PPS−'; N=5). For the last two treatments, a saline solution was used to keep the lungs moist throughout the procedures. Sample size was reduced for treatments because of lung perforations during dissection, or other difficulties during data collection.

Data analysis

From the raw data obtained, we extracted values for maximum lung volume (V_L), resting lung volume (V_{Lr}), C_{stat}, C_{dyn} and work of breathing following the methodologies of Perry and Duncker (1978), Milsom and Vitalis (1984) and Klein et al. (2003). Briefly, V_L was determined as the total amount of air in the respiratory system. V_{Lr} was the amount of air that could be withdrawn from the resting position until a pressure of −10 cmH_2O. C_{stat} was defined as the inclination at the steepest part of the inflation curve. The total static compliance of the respiratory system (C_T, synonymous with the Intact treatment) was the sum of the static compliance of the free lungs (C_L, but here adopted as a synonym for the PPS− treatment) plus the static compliance of the body wall (C_B), such that C_B could be calculated by rearranging the following equation:

$$\frac{1}{C_T} = \frac{1}{C_B} + \frac{1}{C_L}. \quad (1)$$

From this, the percentage of work required to overcome the elastic forces resisting the static inflation coming from the body wall or the lungs was calculated by:

$$\%C_i = \left(1 - \frac{C_i}{C_B + C_L}\right) \times 100, \quad (2)$$

where 'i' is an index for C_B and C_L.

C_{dyn} was defined as the slope of the line connecting the points of zero flow on the different pressure–volume loops. Work per ventilation (W) was obtained by determining the area of a pressure–volume loop that enclosed the inflation curve, a horizontal line connecting the maximum inflation volume with the y-axis, and the y-axis from zero to maximum volume (for reference, see area ABCIA in fig. 3A from Milsom and Vitalis, 1984). These areas were determined by exporting each pressure–volume loop into ImageJ Software (US National Institutes of Health, Bethesda, MD,

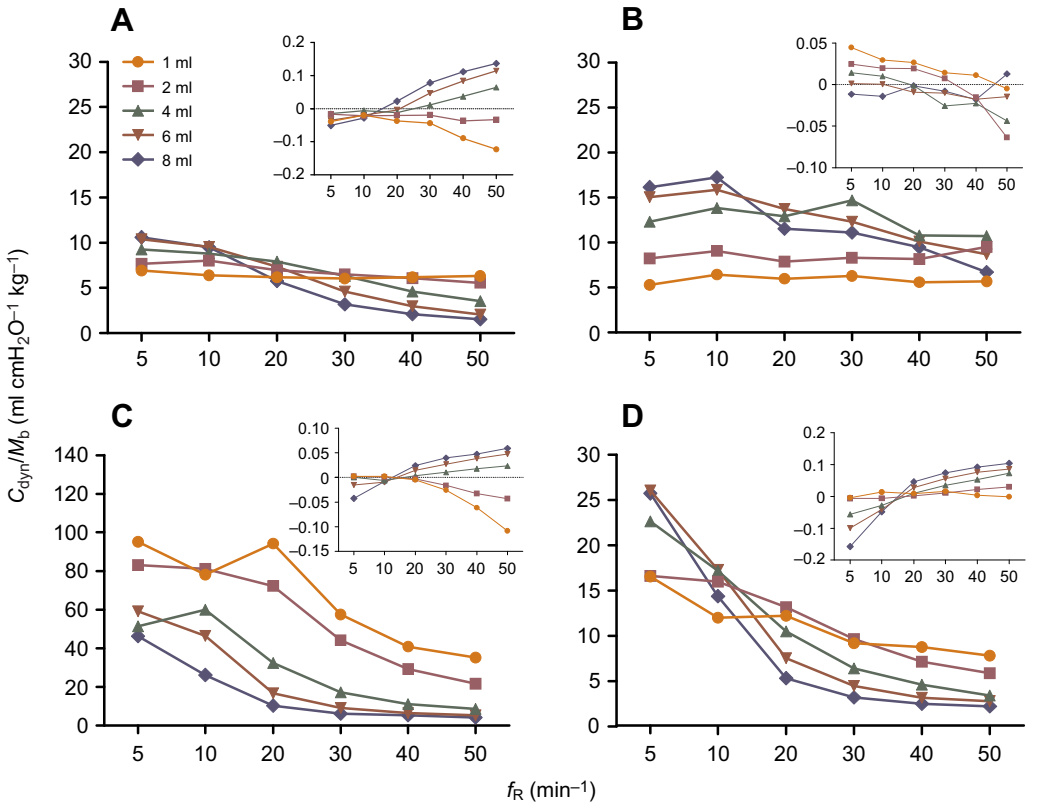

Fig. 2. Mean values of dynamic compliance (C_{dyn}) plotted against ventilatory frequency (f_R) for each treatment. (A) Intact, (B) Submerged, (C) PPS+ and (D) PPS−. Data were separated by the different pump volumes, given in the key. The residual plot for the different treatments is shown in the inset for each graph. The residual plot for the Intact treatment refers to the comparison with the Submerged treatment; the corresponding plot of comparison with PPS treatments is in Fig. S2. Note the different y-axis scale for the PPS+ treatment (C) and for all residual plots.

Journal of Experimental Biology (2021) 224, jeb242386. doi:10.1242/jeb.242386

USA, https://imagej.nih.gov/ij/) and determining the number of pixels in each area. The number of pixels was then transformed into work values (ml cmH_2O ventilation^{-1}) through division by a known area of 1 cm ml.

From W, isopleths were constructed as linear regression lines of $\log_{10}$-transformed work by pulmonary ventilation ($\dot{V}_e$), separated according to the different f_R, with f_R being calculated by dividing $\dot{V}_e$ by V_T. From this, vertical lines referring to pump volumes of 25, 50, 75, 100 and 125 ml min^{-1} were plotted on the same graph, so that the anti-log of the work values for which these lines crossed the isopleths were used to calculate the minute work of breathing ($\dot{W}$ in ml cmH_2O min^{-1} kg^{-1}), which was then plotted against the respiratory frequency and separated according to each of the four levels of ventilation.

Data were statistically analyzed by fitting a generalized estimating equation (GEE) model. Models with Gaussian and Gamma distribution, as different types of covariance matrix were compared, and adjustment of the residuals of each model to a Gaussian Q–Q plot, along with quasi information criterion (QIC) and correlation information criterion (CIC) tests, was used to choose the best model. From this, it was ascertained that the models with a Gamma distribution, an inverse link function, and an AR(1) matrix were the best choice for C_{stat}, while an 'exchangeable' matrix was best for C_{dyn} and W. For C_{stat}, the treatments were the only predictor, while for C_{dyn} and W, treatment, volume and frequency were used as explanatory variables, without considering their interactions. To analyze the effect of submersion, we compared the groups Intact and Submerged, while to analyze the influence of the PPS and the body wall as a whole, we compared the groups Intact, PPS+ and PPS−.

Analyses were carried out on data standardized by body mass (M_b) and a significance level of 0.05 was adopted as an indicator of statistical difference. All data were analyzed in R 3.6.3 and the software Prism 6.0 (GraphPad Software, https://www.graphpad.com/) was used to construct the graphs.

RESULTS

Static compliance

Lung volumes obtained during C_{stat} measurements are given in Table 1. The Intact and Submerged treatments resulted in lower compliance values when compared with those of animals with exposed lungs (Fig. 1). Submersion resulted in a significantly greater C_{stat} when compared with values for Intact animals, while exposure of the lungs significantly increased C_{stat} compared with that for Intact animals (Table S1). The PPS+ group did not generate significantly different C_{stat} when compared with the PPS− group (Table S1). Mean (±s.e.m.) values for C_T (12.28 ±2.03 ml cmH_2O^{-1} kg^{-1}), C_L (42.55±4.37 ml cmH_2O^{-1} kg^{-1}) and C_B (21.69±3.42 ml cmH_2O^{-1} kg^{-1}) showed that C_L was much greater than C_B and C_T.

Dynamic compliance

Changes in volume and frequency resulted in significant effects on C_{dyn} in Intact and Submerged turtles, as well as in animals with exposed lungs (PPS+, PPS−; Tables S2 and S3). Compared with the Intact group, Submerged animals showed significantly different

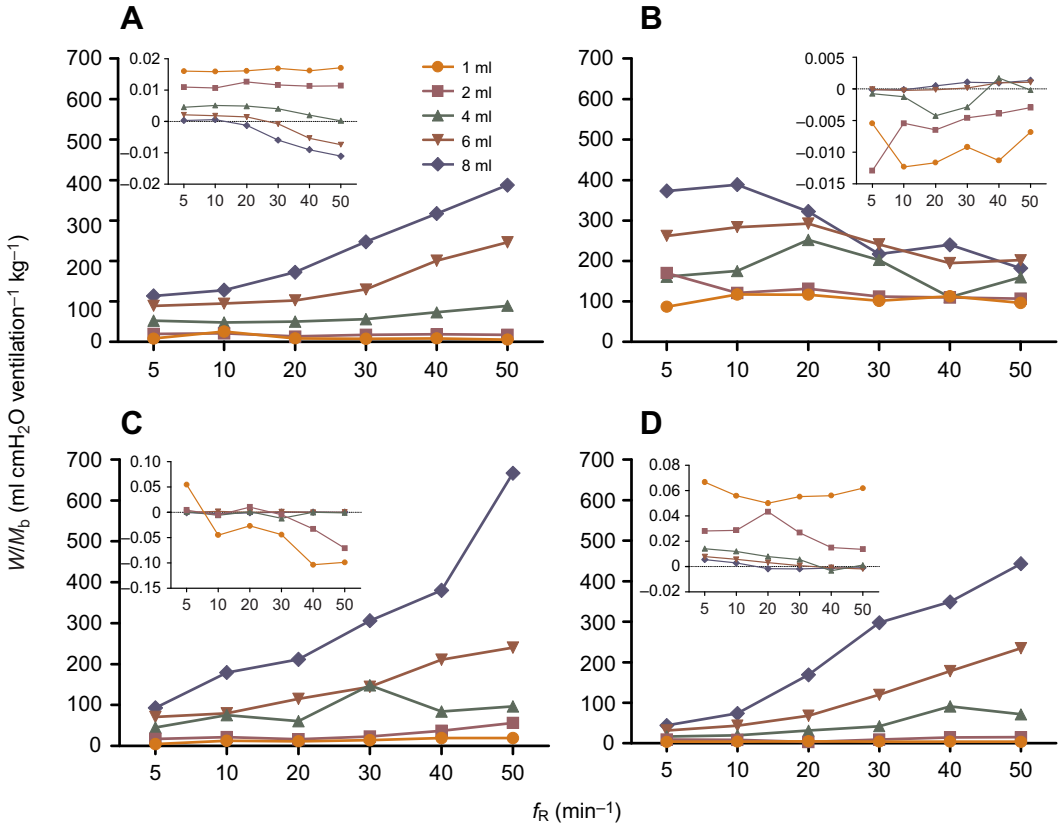

Fig. 3. Mean values of work per ventilation (W) plotted against f_R for each treatment. (A) Intact, (B) Submerged, (C) PPS+ and (D) PPS−. Data were separated by the different pump volumes, given in the key. The residual plot for the different treatments is shown in the inset for each graph. The residual plot for the Intact treatment refers to the comparison with the Submerged treatment; the corresponding plot of comparison with PPS treatments is in Fig. S2. Symbols used as in Fig. 2. Note the different y-axis scale for all residual plots.

Journal of Experimental Biology (2021) 224, jeb242386. doi:10.1242/jeb.242386

C_{dyn} overall, as well as at all volumes and several frequencies tested (Fig. 2; Table S3). Exposure of the respiratory system (PPS+, PPS−) generated significantly different C_{dyn} compared with that of Intact animals, while removal of the PPS resulted in a significantly lower C_{dyn} in PPS− animals when compared with the PPS+ group (Table S3).

The changes in V_T and f_R had a significant influence on C_{dyn} so that the increase in frequency led to a tendency to decrease compliance, mostly at greater volumes. While an increase in volume generated an increase in C_{dyn} at low frequencies for Intact, Submerged and PPS− treatments, at greater frequencies in the Intact, PPS+ and PPS− treatments, and at low frequencies in the PPS+ group, C_{dyn} decreased with increasing volume. The influence of frequency was more accentuated in the treatments assessing the compliance of the lungs (PPS+ and PPS−), which showed a large initial drop with increasing frequency until reaching a state of minor variation, maintaining low C_{dyn} at greater frequencies, with a greater distinction between volumes in the PPS+ treatment (Fig. 2).

Work of breathing

For all groups, significant effects of volume and frequency on W were detected (Table S2). Submersion did not generated a significant influence on W when compared with Intact animals (P=0.83; Table S4). Exposure of the respiratory system also did not result in a significant difference in W between the Intact, PPS+ and PPS− groups, nor between the PPS− and PPS+ groups (Table S4).

The changes in V_T and f_R had a significant influence on W so that, for the Intact, PPS+ and PPS− treatments, the increase in both led to a tendency to increase W, especially at larger volumes (Fig. 3; Table S4). This increase is better illustrated in Fig. 4, which shows W plotted against $\dot{V}_e$ on log–log scales, separated according to volume and frequency. A more pronounced effect on W can be seen with increasing volume than with increasing frequency in the Intact, PPS+ and PPS− groups, where at low frequencies only small increases in W occurred, while at frequencies of 30, 40 and 50 min^{-1}, greater increases were observed. For the Submerged treatment, a different pattern was found. At smaller volumes, little influence of frequency was observable, while at greater volumes the increase in frequency led to a tendency to decrease W (Fig. 4B). In Submerged animals, W at small volumes was always greater than that in Intact animals, independent of frequency, while at volumes of 6 and 8 ml and frequencies of 30, 40 and 50 min^{-1}, W was greater than in the corresponding Intact animals.

The isopleths constructed for W were not parallel, but showed greater inclinations at higher frequencies, especially in the Intact and PPS− groups (Fig. 5). The values obtained from Fig. 5 are presented in Fig. 6, which shows $\dot{W}$ against f_R. These curves show a greater influence of the level of pulmonary ventilation than frequency on work for the Intact and PPS− treatments, while for the Submerged treatment a clear increase in $\dot{W}$ can be observed with increasing frequency. For PPS+, a roughly U-shaped curve was obtained at higher ventilations, revealing a more complex relationship between frequency, ventilation and $\dot{W}$ when compared with the other treatments.

DISCUSSION

Static compliance

The C_{stat} results obtained in this study follow the published data for turtles, as shown in Table 2. As expected, the C_B obtained in this

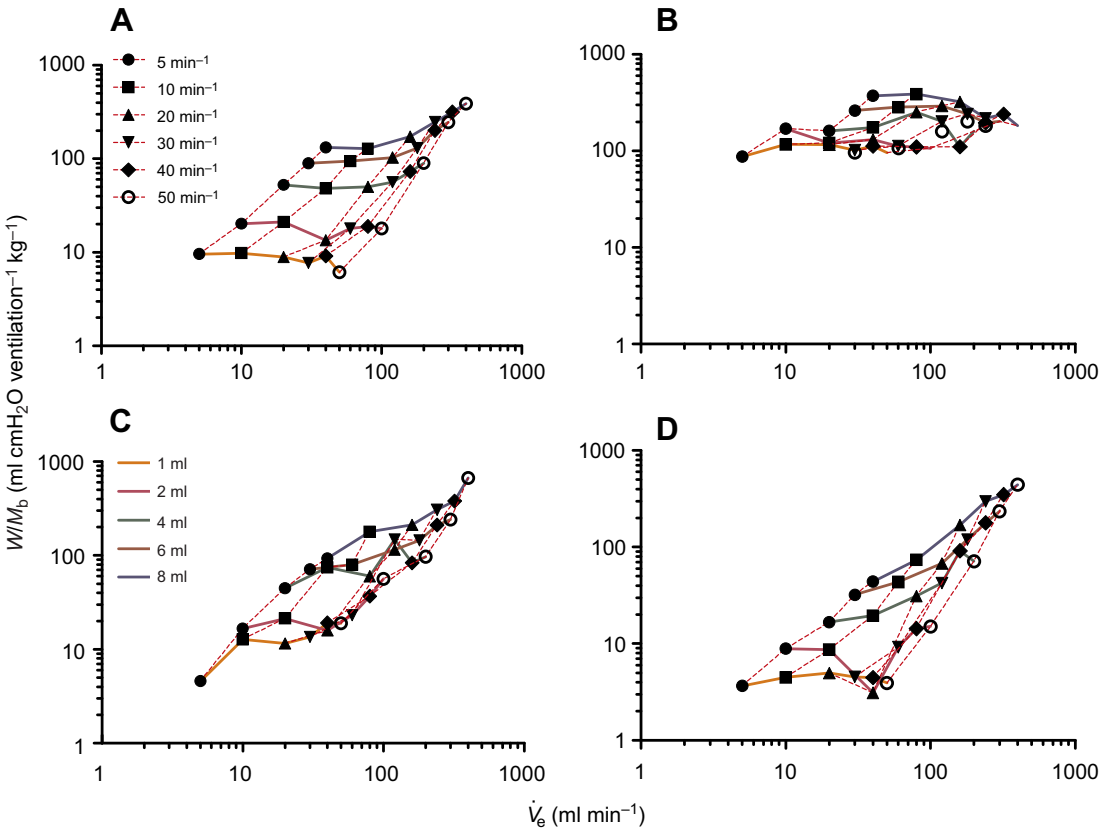

Fig. 4. Mean values of work per ventilation (W) against pulmonary ventilation ($\dot{V}_e$) for each treatment. (A) Intact, (B) Submerged, (C) PPS+ and (D) PPS−. Data are plotted on double logarithmic scales; the different ventilation frequencies and pump volumes used are indicated in the keys in A and C and apply to all panels.

Journal of Experimental Biology (2021) 224, jeb242386. doi:10.1242/jeb.242386

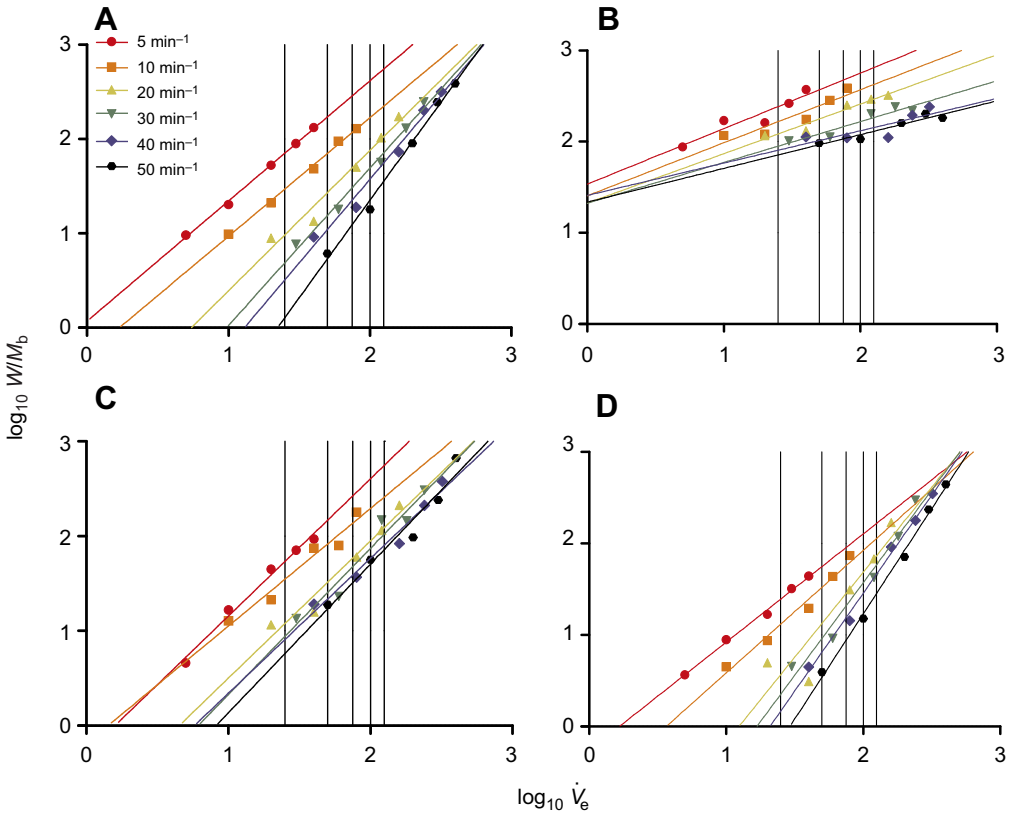

Fig. 5. Linear regression of W plotted against $\dot{V}_e$ for each treatment. (A) Intact, (B) Submerged, (C) PPS+ and (D) PPS−. Data for W (ml cmH_2O ventilation^{-1} kg^{-1}) and $\dot{V}_e$ (ml min^{-1}) were $\log_{10}$ transformed; data are separated by the different ventilation frequencies, given in the key. The vertical lines indicate ventilation of (from left to right) 25, 50, 75, 100 and 125 ml min^{-1}.

study reflects the relative rigidity that has been attributed to the turtle shell, although the values for C_B found here were somewhat greater than those obtained in other studies, and are greater than those obtained for adult *Caiman yacare*, *Crocodylus niloticus* and *Gekko gecko* (Table 2). Table 3 shows the percentage of the work required to overcome the elastic forces resisting the static inflation of the lung coming from the body wall or the lungs. The expected pattern for reptiles is obtained, in which the body wall offers most of the elastic resistance (Vitalis and Milsom, 1986a); however, the resistance offered by the body wall was found in the present study to be less than that found in other studies on the same species. This could be related to the size of the specimens analyzed here, as the deformability of the carapace of *T. scripta* turtles decreases with growth, which may be the product of an increase in the degree of mineralization or thickness of the shell (Fish and Stayton, 2014). Looking at juveniles and adults of *Caiman yacare*, Reichert et al. (2019) also found a difference in their compliance, with juveniles presenting a greater C_B than adults, which could reflect the lack of osteoderms and a lower degree of muscle mass and keratinization of the body wall in young caimans.

Dynamic compliance and work of breathing

C_{dyn} in the Intact group showed a similar magnitude and pattern to those described in the literature; however, a greater dependency on volume and frequency was found in the present study. Although we found C_{dyn} to be greatest at the lowest frequency and to decrease with increasing frequency, as shown by Vitalis and Milsom (1986a), this was not true for the lower volumes tested, mostly 1 and 2 ml, where C_{dyn} remained unchanged with increasing frequency. These differences might be explained by the fact that the animals used by Vitalis and Milsom (1986a) had double the body mass of the animals used in the present study and, furthermore, the pump volumes used by Vitalis and Milsom (1986a) ranged from 1.8 to 10.8 ml kg^{-1}, whereas in this study pump volumes ranged from 4.3 to 34.8 ml kg^{-1}. As resting V_T in normoxic normocarbic breathing *T. scripta* ranges between 20 and 30 ml kg^{-1} (Trevizan-Baú et al., 2018), the present study explored breathing mechanics by simulating V_T comparable to those of undisturbed animals. This allowed a better evaluation of the effect of ventilation volume on C_{dyn}, finding a greater influence of volume, just as has been described by Milsom and Vitalis (1984) for tokay geckos. Interestingly, we found an inversion of volume with increasing frequency: at low frequencies, C_{dyn} increased with increasing volume, while at the greatest frequencies, C_{dyn} decreased with increasing volume, and the inversion took place around 20 min^{-1}. A similar pattern was observed in the PPS− group, but at a frequency of 10 min^{-1} (Fig. 2). As the decrease in C_{dyn} with increasing frequency is related to an increase in the stiffness of the lungs (Vitalis and Milsom, 1986a), according to Laplace's law, an increase in volume would reduce the apparent stiffness of the lung; however, this would be compensated for by a decreasing elasticity of the organ at larger volumes (Milsom and Vitalis, 1984). Thus, greater pressure changes would be necessary to produce the same volume change at greater frequencies (Reichert et al., 2019), which would generate the need for more work as the volume increases, especially at greater frequencies.

The results obtained for W in Intact animals and the PPS+ and PPS− groups showed an increase with increasing volume, being

Journal of Experimental Biology (2021) 224, jeb242386. doi:10.1242/jeb.242386

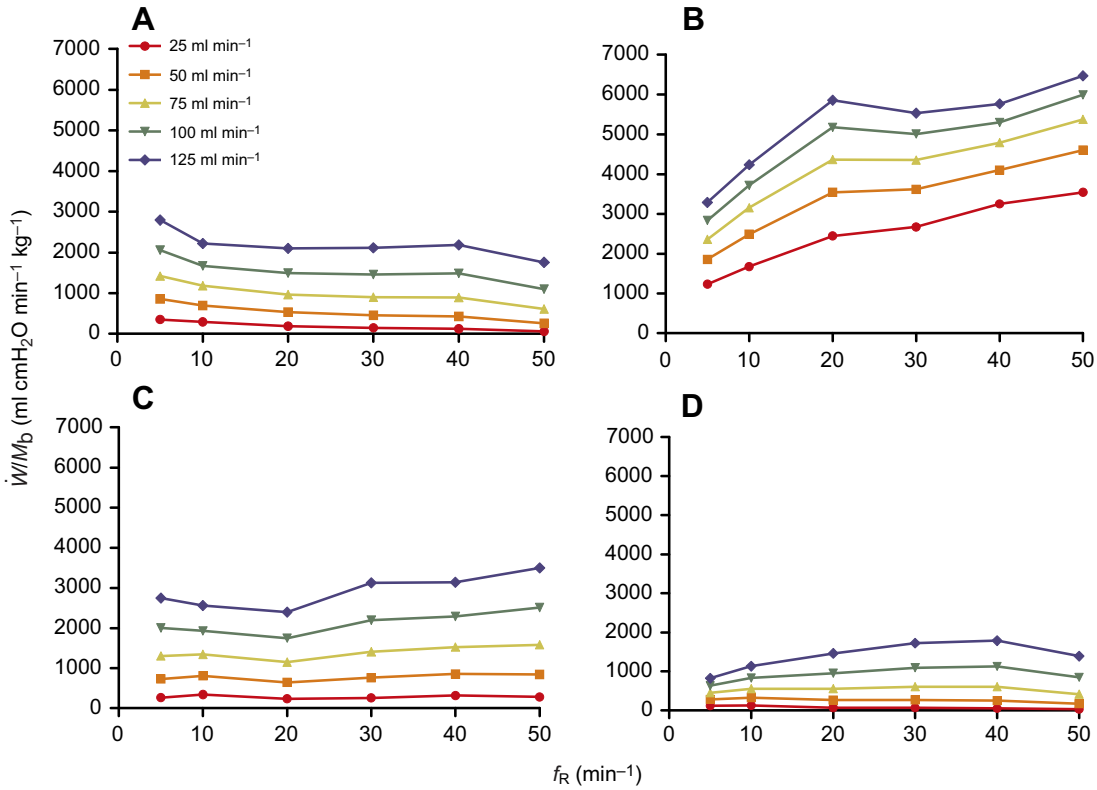

Fig. 6. Minute work of breathing ($\dot{W}$) plotted against f_R for each treatment. (A) Intact, (B) Submerged, (C) PPS+ and (D) PPS−. $\dot{W}$ was derived from regressions given in Fig. 5. Data were separated by different $\dot{V}_e$, given in the key.

exacerbated by increasing frequency (Fig. 3). These results are coherent with the patterns observed for C_{dyn}, stiffer systems needing more work to be ventilated, and in addition are similar to the patterns described in the literature for *G. gecko* (Milsom and Vitalis, 1984), *C. yacare* (Reichert et al., 2019) and *T. scripta* (Vitalis and Milsom, 1986a).

While Intact animals showed $\dot{W}$ to be greatest at 5 min^{-1} and smallest at 50 min^{-1}, PPS− lungs showed the lowest values of minute work, with little or no influence of ventilation frequency, suggesting that the body wall and the PPS are the main factors defining the relationship between minute work and ventilatory frequency (Fig. 6). With the graphs generated, it is also possible to evaluate the frequency responsible for generating the least mechanical work; however, the pattern obtained here for Intact animals differs greatly from the U-shaped curves presented for turtles of the same species by Vitalis and Milsom (1986a) and for

Table 2. Values of total static compliance (C_T), body wall compliance (C_B) and lung compliance (C_L) standardized by body mass (C_{stat}/M_b) of reptiles

Order	Species	M_b (kg)	C_T (ml cmH_2O^{-1} kg^{-1})	C_B (ml cmH_2O^{-1} kg^{-1})	C_L (ml cmH_2O^{-1} kg^{-1})	Reference
Testudines						
	Caretta caretta	30.1	10.7	13.7	41.7	Lutcavage et al., 1989
	Mauremys caspica	0.2	15.3	–	–	Pages et al., 1990
	Trachemys scripta	0.2–0.6	10.0	10.6	170.0	Jackson, 1971
	Trachemys scripta	0.7	8.4	11.6	35.1	Vitalis and Milsom, 1986a,b
	Trachemys scripta	0.2	12.2	21.69	42.5	This study
	Trachemys scripta (submerged)	0.2	13.3	33.2	42.5	This study
Crocodylia						
	Caiman yacare (juvenile)	0.03	28.9	33.9	154	Reichert et al., 2019
	Caiman yacare (adult)	27.9	12.0	16.7	42.5	Reichert et al., 2019
	Crocodylus niloticus	4.1	12.3	10.6	73.9	Perry, 1988
Squamata						
	Chamaeleo chamaeleo	0.0	306	512.0	759.0	Perry and Duncker, 1978
	Gekko gecko	0.1	47.0	57.0	273.0	Perry and Duncker, 1978
	Gekko gecko	0.1	16.0	15.0	202.0	Milsom and Vitalis, 1984
	Lacerta viridis	0.0	18.0	27.0	62.0	Perry and Duncker, 1978
	Tupinambis merianae	0.7	23.1	39.7	90.7	Klein et al., 2003
	Varanus exathematicus	0.2	67.0	82.0	36.0	Perry and Duncker, 1978

C_{stat}, static pulmonary compliance.

Journal of Experimental Biology (2021) 224, jeb242386. doi:10.1242/jeb.242386

Table 3. Percentage of total work required to overcome the elastic forces resisting the static inflation of the lungs associated with either the body wall or the lungs

Order	Species	Total work (%)		Reference
		Body wall	Lungs	
Testudines				
	Caretta caretta	75	25	Lutcavage et al., 1989
	Trachemys scripta	94	6	Jackson, 1971
	Trachemys scripta	75	25	Vitalis and Milsom, 1986a,b
	Trachemys scripta	66	34	This study
	T. scripta (submerged)	56	44	This study
Crocodylia				
	Caiman yacare (juvenile)	82	18	Reichert et al., 2019
	Caiman yacare (adult)	72	28	Reichert et al., 2019
	Crocodylus niloticus	87	13	Perry, 1988
Squamata				
	Chamaeleo chamaeleo	60	40	Perry and Duncker, 1978
	Gekko gecko	83	17	Perry and Duncker, 1978
	Gekko gecko	93	7	Milsom and Vitalis, 1984
	Lacerta viridis	70	30	Perry and Duncker, 1978
	Tupinambis merianae	70	30	Klein et al., 2003
	Varanus exathematicus	82	18	Perry and Duncker, 1978

Data were calculated based on C_{stat} standardized by M_b.

C. yacare by Reichert et al. (2019). Such a discrepancy may be explained by the fact that we did not test frequencies above 50 min^{-1} as in the previous studies. Furthermore, W did not behave in the same manner with increasing ventilation as seen in other studies. While W in *G. gecko*, *T. scripta* and *C. yacare* behaves roughly similarly at each frequency tested when plotted against ventilation (Milsom and Vitalis, 1984; Vitalis and Milsom, 1986a; Reichert et al., 2019), in the present study, the same plot (Fig. 5) resulted in non-parallel isopleths, due to a great increase in W at volumes of 4, 6 and 8 ml and frequencies of 30, 40 and 50 min^{-1}. Fig. 7 shows the relative change of W derived from data plotted in Fig. 4. To investigate the effect of either an increase in volume or an increase in frequency on W, we calculated for every volume applied the percentage change in work when frequency increased (Fig. 7A), and for every frequency applied the percentage change in work when volume increased (Fig. 7B). It seems evident that, in all treatments, changes in frequency at any volume resulted in only minor changes in W, whereas changes in volume, with the exception of the Submerged group, mostly doubled W with every increment of volume. In particular, an increase from 2 to 4 ml increased W 3- to 5-fold in the Intact, PPS+ and PPS− groups.

Influence of submersion

Only Reichert et al. (2019), studying ventilatory mechanics of submerged *C. yacare* juveniles, have investigated the effect of submersion on ventilatory mechanics in a reptile. They found no difference in C_{stat} between emerged and submerged animals, while C_{dyn} was significantly reduced and W significantly increased with immersion, mainly at the steepest floatation angle, at a hydrostatic pressure of about 5 cmH_2O.

The statistical analysis suggested that submersion significantly increased C_{stat} and decreased C_{dyn}, but did not significantly affect W. The last seems contradictory, as $\dot{W}$ (Fig. 6B) showed greater values in Submerged when compared to Intact animals. The analytical approach to model the distribution of data independently for each treatment and combination of volume and frequency was applied here for the first time to data on breathing mechanics, and the obtained residuals provided support for the differences found (Fig. 3A,B). While the mean values given for C_{dyn} in Fig. 2B suggest a tendency to increase with submergence, the corresponding residuals showed a tendency to decrease with increasing frequency, and were mostly smaller than the residuals found for the Intact treatment, which also showed a greater dispersion for positive values at higher volumes and frequencies. Compared with Intact animals, hydrostatic pressure seemed to result in greater C_{dyn} at the greater volumes used. As shown by Jackson (1971), changes in body cavity volume can significantly alter C_{stat} in *T. scripta*, but the hydrostatic pressure applied to our animals might not have been enough to push the soft body parts inwards sufficiently to impact the respiratory system. Furthermore, the limbs were floating freely in the water, possibly offering less resistance to lung inflation and explaining the differences seen in C_{dyn} between Intact and Submerged animals.

While hydrostatic pressure might or might not aid in passive exhalation by pushing the viscera into the body cavity, during inspiration the animal must exert a greater contractile force by the inspiratory muscles to actively increase the volume of the abdominal cavity, resulting in increased mechanical work of breathing (Gaunt and Gans, 1969). As evidenced by mean values of W (Fig. 3B), with the exception of the greatest volumes and frequencies, work per ventilation was greater in Submerged animals than in Intact ones, resulting in small relative changes in W due to the increase in volume (Fig. 7)

Submerged *T. scripta* show an instantaneous breathing frequency (f) of about 22 breaths min^{-1} under normoxic conditions (Trevizan-Baú et al., 2018). When challenged by either hypoxia or hypercarbia, f tended to decrease (down to roughly 18 breaths min^{-1}), while V_T increased from about 20 ml kg^{-1} up to about 60 ml kg^{-1} (Trevizan-Baú et al., 2018). As overall breathing frequency only showed a small tendency to increase from 1 to 2 breaths min^{-1}, the resulting minute ventilation increased from resting values of 16–20 ml min^{-1} kg^{-1}, up to 116.5 ml min^{-1} kg^{-1} at 3% O_2, or 215.9 ml min^{-1} kg^{-1} at 6.0% CO_2 (Trevizan-Baú et al., 2018). The large increase in V_T observed under both hypoxia and hypercarbia might represent a compromise between efficient lung ventilation and mechanical cost of ventilation (Vitalis and Milsom, 1986b). Despite increasing volumes resulting in greater W for any given frequency (Fig. 3), a turtle should not

Journal of Experimental Biology (2021) 224, jeb242386. doi:10.1242/jeb.242386

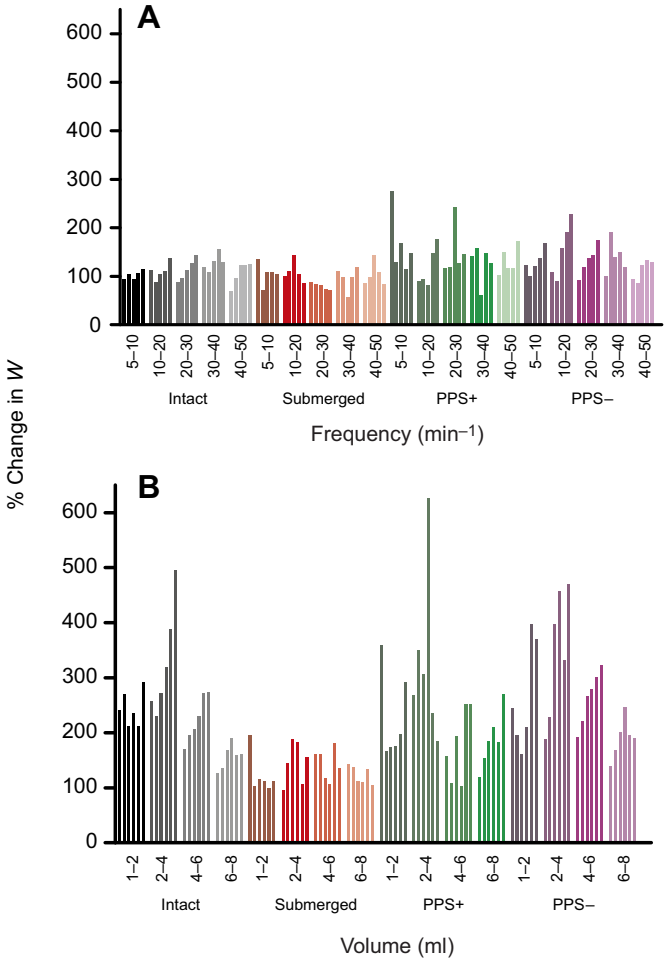

Fig. 7. Percentage change in *W* for the different treatments. (A) Relative change in *W* (derived from data given in Fig. 4) caused by an increase in frequency (increase in frequency from 5 to 10, 10 to 20, 20 to 30, 30 to 40, and 40 to 50 min^{-1}), for the different volumes (from left to right within each frequency dataset: 1, 2, 4, 6, 8 ml). (B) Relative change in *W* (derived from data given in Fig. 4) caused by an increase in volume (increase in volume from 1 to 2, 2 to 4, 4 to 6, and 6 to 8 ml), for the different frequencies (from left to right within each volume dataset: 5, 10, 20, 30, 40, 50 min^{-1}).

ventilate at low volumes and high frequencies, as such a breathing pattern would increase dead-space ventilation and thereby reduce the transport of fresh air to the respiratory surfaces (Vitalis and Milsom, 1986b). The decrease in f observed in conscious submerged animals when ventilatory demand increased might be explained by the great decrease in minute work observed in the present study when frequency decreased from 20 to 10 min^{-1} (Fig. 6B). Analysis of work per breath in submerged animals (Fig. 3B) actually suggests that increasing frequency did not increase *W*, unlike in Intact animals. This could indicate that submerged turtles might be able to ventilate their respiratory system at a given volume and with frequencies between 20 and 40 min^{-1} without significantly increasing the mechanical cost of ventilation (Fig. 6B). Interestingly, *Podocnemis unifilis*, a semiaquatic turtle with very similar habits to *T. scripta*, did show a very great increase in breathing frequency (from about 2 to 16 breaths min^{-1}) and only a moderate increase in V_T (10 to 18 ml kg^{-1}) when challenged with hypercarbia while submerged (Cordeiro et al., 2016). The breathing mechanics of *P. unifilis*, however, has yet to be investigated.

Influence of the PPS

Few studies have evaluated the influence of intracoelomic septa on the ventilatory mechanics of reptiles. In the tegu lizard, the removal of the post-hepatic septum (PHS), without removing any other organ, led to a decrease in C_{stat} (Klein et al., 2003), while in the present study, the removal of the turtle PPS led to a decrease in C_{dyn}, but did not significantly affect C_{stat} and *W*. While the results found for the tegu lizard occurred as a result of displacement of the viscera towards the pleuro-hepatic cavity, previously delimited by the PHS, reducing the space for lung expansion (Klein et al., 2003), in turtles, the PPS may act to stabilize the heterogeneous structure of the lung, preventing preferentially collapse of the denser cranial and central regions (Perry and Duncker, 1980). While C_{stat} did not show a significant change as a result of removal of the PPS, C_{dyn} was considerably lower in the PPS− group at lower volumes and especially at frequencies ranging from 5 to 30 min^{-1} (Fig. 2). The greatest volumes tested tended to show a similarly low C_{dyn} at frequencies of 40 and 50 min^{-1} in PPS+ and PPS− treatments; for example, at 8 ml and 50 min^{-1}, C_{dyn} was 2.24 ml cmH_2O^{-1} kg^{-1} for the PPS− and 4.19 ml cmH_2O^{-1} kg^{-1} for the PPS+ treatment (Fig. 2).

Contrary to the frequency-dependent inversion in C_{dyn} seen in PPS− animals, in the PPS+ group, the smallest volumes always produced the greatest compliance and increasing volumes decreased C_{dyn} at every frequency. These results suggest that the PPS not only acts by increasing the compliance of the isolated respiratory system but also seems to change the overall mechanical response of the respiratory system to changes in volume and frequency.

Functionally, the PPS of *T. scripta* seems to maintain the cranial and central part of the respiratory system in a partially expanded state, and within this volume, small volumes of air may easily be moved without the interference of the viscera. The decrease in C_{dyn} in PPS− animals could be explained according to Laplace's law, where geometric changes resulting from an increase in lung volume result in an apparent decrease in the rigidity of the respiratory system (Milsom and Vitalis, 1984). The opposite may have occurred with the removal of the PPS, collapsing pulmonary structures, decreasing the size of pulmonary chambers, leading to an increase in the apparent rigidity of the system, and decreasing C_{dyn}. Thus, the PPS seems to maintain the structural integrity of the lung within a given volume of the body cavity, reducing its apparent stiffness.

Regarding work per ventilation (Fig. 3), only at the greatest volume (8 ml) was *W* much larger in the PPS+ group, especially at the greatest frequency. Our hypothesis for the unexpectedly greater *W* at 8 ml in lungs with intact PPS might be related to a possible deformation of the carapace once the plastron had been removed. The relatively young individuals used here might not have possessed a sufficiently ossified carapace to maintain the angle of the carapace with the vertebral column. The resulting increase in carapace width would extend the PPS, increasing its tension, as it is fixed to the inner lining of the carapace. A PPS stretched in such a way could thus increase the work required to move it at large ventilation volumes. At small volumes, the caudal part of the lungs not covered by the PPS would expand, offering little resistance, but at the greatest volume used, the caudal expansion of the lungs would be maximal and the PPS would need to move ventrally to account for increased lung volume, resulting in greater work due to the tensioned PPS. As in the intact animal the PPS would not be stretched in the hypothesized manner, the work necessary to move the viscera during ventilatory movements seems to be less when compared with that for lungs with intact PPS. If this is actually the case, it would show how variation in the tension of an intracoelomic septum might influence breathing mechanics.

The PPS of *T. scripta* possesses skeletal muscle fibers (von Hansemann, 1915; Perry and Sander, 2004), suggesting that turtles might be able to change the tension of the PPS by contracting or relaxing these muscles, thereby possibly changing the work of breathing. A similar function has being envisaged for the costopulmonary muscles of the avian horizontal septum (a derivative of the PPS; Duncker, 1979), which originate at the ribs and insert into the horizontal septum, and supposedly act to maintain the space occupied by parabronchi at a constant volume during ventilatory movements of the thoracic cavity (Duncker, 2004). Our data on minute work provide further evidence for the idea of a stretched PPS following removal of the plastron, as the greatest work values were obtained for ventilation at the greatest frequency and for the greatest level of ventilation (Fig. 6C).

A PPS as studied here in *T. scripta* is present in several species of chelonians, but shows varying degrees of completeness in the taxon. In sea turtles (*Chelonia mydas* and *Caretta caretta*), the PPS is well developed, just as in the terrestrial *Testudo hermanni* and in the semi-aquatic *Lissemys punctata*, where it is also well muscularized. The primarily terrestrial *Terrapene carolina* shows a reduced PPS, while in the aquatic bottom-walking *Chelydra serpentina* and in the terrestrial *Testudo graeca* it is absent (Lambertz et al., 2010; Perry, 1998; Perry and Sander, 2004). It seems evident that the functional advantages of a PPS (increased dynamic compliance, possibility to maintain a constant volume for the lungs within the body cavity, altering the tension of the PPS through muscular contraction) may be correlated either to the phylogenetic history or the lifestyle of testudines. A correlation between PPS morphology and chelonian phylogeny and lifestyle seems fundamental to understanding the evolution of this structure within this taxon.

In conclusion, the present study provides evidence for the greater mechanical work needed in submerged *T. scripta* as a result of the hydrostatic pressure acting upon the flexible parts of the animal's body wall. Any level of ventilation resulted in a much greater amount of minute work, especially at physiologically relevant breathing frequencies. Similarly, we show for the first time how a PPS affects the breathing mechanics of a respiratory system in a chelonian, providing evidence that even a PPS not completely separating the lungs from the remaining viscera is able to influence significantly the mechanics of the respiratory system.

Acknowledgements
We thank Augusto S. Abe for providing the animals used in the current study.

Competing interests
The authors declare no competing or financial interests.

Author contributions
Conceptualization: R.B.B.d.S., W.K.; Methodology: R.B.B.d.S., W.K.; Validation: R.B.B.d.S., W.K.; Formal analysis: R.B.B.d.S., W.K.; Investigation: R.B.B.d.S., W.K.; Resources: R.B.B.d.S., W.K.; Data curation: R.B.B.d.S., W.K.; Writing - original draft: R.B.B.d.S., W.K.; Writing - review & editing: R.B.B.d.S., W.K.; Visualization: R.B.B.d.S., W.K.; Supervision: W.K.; Project administration: R.B.B.d.S., W.K.; Funding acquisition: W.K.

Funding
R.B.B.d.S. was supported by Fundação de Amparo à Pesquisa do Estado de São Paulo (FAPESP; process no. 2020/01289-8) and W.K. thanks the Conselho Nacional de Desenvolvimento Científico e Tecnológico (CNPq) for funding (process no. 308249/2019-4).

References
Cordeiro, T. E. F., Abe, A. S. and Klein, W. (2016). Ventilation and gas exchange in two turtles: *Podocnemis unifilis* and *Phrynops geoffroanus* (Testudines: Pleurodira). *Respir. Physiol. Neurobiol.* **224**, 125-131. doi:10.1016/j.resp.2014.12.010

Crosfill, M. L. and Widdicombe, J. G. (1961). Physical characteristics of the chest and lungs and the work of breathing in different mammalian species. *J. Physiol.* **158**, 1-14. doi:10.1113/jphysiol.1961.sp006750

Duncker, H. R. (1979). General morphological principles of amniotic lungs. In *Respiratory Function in Birds, Adult and Embryonic* (ed. J. Piiper), pp. 2-15. Springer.

Duncker, H. R. (2004). Vertebrate lungs: Structure, topography and mechanics. A comparative perspective of the progressive integration of respiratory system, locomotor apparatus and ontogenetic development. *Respir. Physiol. Neurobiol.* **144**, 111-124. doi:10.1016/j.resp.2004.07.020

Fish, J. F. and Stayton, C. T. (2014). Morphological and mechanical changes in juvenile red-eared slider turtle (*Trachemys scripta elegans*) shells during ontogeny. *J. Morphol.* **275**, 391-397. doi:10.1002/jmor.20222

Gaunt, A. S. and Gans, C. (1969). Mechanics of respiration in the snapping turtle, *Chelydra serpentina* (Linné). *Journaul Morphol.* **128**, 195-228. doi:10.1002/jmor.1051280205

Jackson, D. C. (1971). Mechanical basis for lung volume variability in the turtle *Pseudemys scripta elegans*. *Amer. J. Physiol.* **220**, 754-758. doi:10.1152/ajplegacy.1971.220.3.754

Klein, W. and Owerkowicz, T. (2006). Function of intracoelomic septa in lung ventilation of amniotes: lessons from lizards. *Physiol. Biochem. Zool.* **79**, 1019-1032. doi:10.1086/507656

Klein, W., Abe, A. S. and Perry, S. F. (2003). Static lung compliance and body pressures in *Tupinambis merianae* with and without post-hepatic septum. *Respir. Physiol. Neurobiol.* **135**, 73-86. doi:10.1016/S1569-9048(03)00063-6

Lambertz, M., Böhme, W. and Perry, S. F. (2010). The anatomy of the respiratory system in Platysternon megacephalum Gray, 1831 (Testudines: Cryptodira) and related species, and its phylogenetic implications. *Comp. Biochem. Physiol. A Mol. Integr. Physiol.* **156**, 330-336. doi:10.1016/j.cbpa.2009.12.016

Lutcavage, M. E., Lutz, P. L. and Baier, H. (1989). Respiratory mechanics of the loggerhead sea turtle. *Caretta caretta. Resp. Physiol.* **76**, 13-24.

Lyson, T. R., Schachner, E. R., Botha-Brink, J., Scheyer, T. M., Lambertz, M., Bever, G. S., Rubidge, B. S. and De Queiroz, K. (2014). Origin of the unique ventilatory apparatus of turtles. *Nat. Commun.* **5**, 5211. doi:10.1038/ncomms6211

Milsom, W. K. and Vitalis, T. Z. (1984). Pulmonary mechanics and the work of breathing in the lizard, Gekko gecko. *J. Exp. Biol.* **113**, 187-202. doi:10.1242/jeb.113.1.187

Pages, T., Fuster, J. F. and Palacios, L. (1990). Some mechanical characteristics of the respiratory system of the fresh-water turtle *Mauremys caspica*. *Comp. Biochem. Physiol.* **97**3, 411-416.

Perry, S. F. (1983). Reptilian lungs: functional anatomy and evolution. *Adv. Anat. Embryol. Cell Biol.* **79**, 81. doi:10.1007/978-3-642-68964-2

Perry, S. F. (1988). Functional morpholgy of the lungs of the nile crocodile, *Crocodylus niloticus*: non-respiratory parameters. *J. Exp. Biol.* **97**, 99–117.

Perry, S. F. (1998). Lungs: Comparative Anatomy, Functional Morphology, and Evolution. In *Biology of Reptilia: (Morphology G)*, Vol. 19 (ed. C. Gans and A. S. Gaunt), pp. 1-93. Ithaca: Society for the Study of Amphibians and Reptiles.

Perry, S. F. and Duncker, H.-R. (1978). Lung architecture, volume and static mechanics in five species of lizards. *Respir. Physiol.* **34**, 61-81. doi:10.1016/0034-5687(78)90049-X

Perry, S. F. and Duncker, H. R. (1980). Interrelationship of static mechanical factors and anatomical structure in lung evolution. *J. Comp. Physiol. B Biochem. Syst. Environ. Physiol.* **138**, 321-334. doi:10.1007/BF00691567

Perry, S. F. and Sander, M. (2004). Reconstructing the evolution of the respiratory apparatus in tetrapods. *Respir. Physiol. Neurobiol.* **144**, 125-139. doi:10.1016/j.resp.2004.06.018

Reichert, M. N., Oliveira, P. R. C., Souza, G. M. P. R., Moranza, H. G., Restan, W. A. Z., Abe, A. S., Klein, W. and Milsom, W. K. (2019). The respiratory mechanics of the yacare caiman (*Caiman yacare). J. Exp. Biol.* **222**, jeb193037. doi:10.1242/jeb.193037

Trevizan-Baú, P., Abe, A. S. and Klein, W. (2018). Effects of environmental hypoxia and hypercarbia on ventilation and gas exchange in Testudines. *PeerJ* **2018**, 1-27. doi:10.7717/peerj.5137

von Hansemann, D. (1915). Die Lungenatmung der Schildkröten. *Sitzungsberichte der königlich Preuss. Akad. der Wissenschaften* **III-I**, 661-672.

Vitalis, T. Z. and Milsom, W. K. (1986a). Pulmonary mechanics and the work of breathing in the semi-aquatic turtle, Pseudemys scripta. *J. Exp. Biol.* **125**, 137-155. doi:10.1242/jeb.125.1.137

Vitalis, T. Z. and Milsom, W. K. (1986b). Mechanical analysis of spontaneous breating in the semi-aquatic turtle, Pseudemys scripta. *J. Exp. Biol.* **125**, 157-171. doi:10.1242/jeb.125.1.157

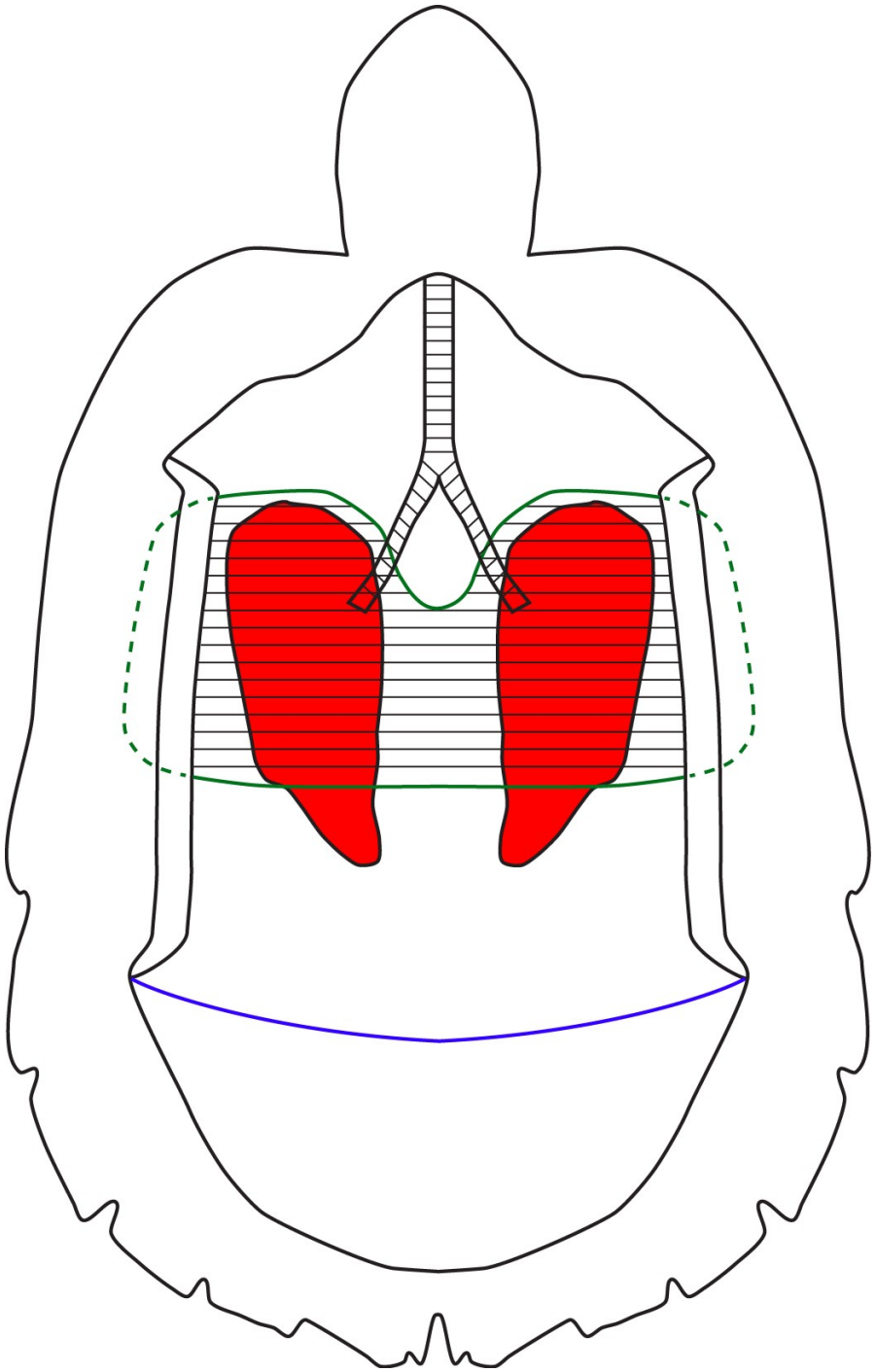

Figure S1. Schematic drawing of the respiratory system (trachea, bronchi, lungs) and the attached post-pulmonary septum (PPS) in *Trachemys scripta*. The drawing is based on a dissected juvenile animal after removal of the plastron, the integument, the legs, and all the viscera except for the respiratory system and the PPS. The lungs were in the collapsed state and are pictured in red. The approximate extension of the PPS, which covers the ventral side of the lungs, is represented by the striped area enclosed within the green line. The caudal-most parts of both lungs are not covered by the PPS and are in direct contact with the organs in the abdominal cavity. The blue line marks the caudal end of the body cavity and caudally to this line, one finds the pelvic girdle, muscles, tail and associated structures.

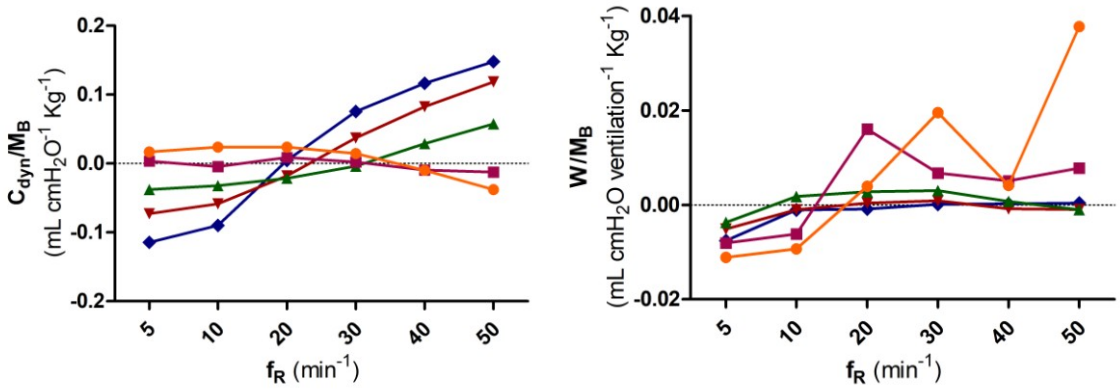

Figure S2. Residual plots for dynamic compliance (C_{dyn}) and work of breathing (W) for the 'Intact' treatment, used in the statistical analysis to be compared to the post-pulmonary septum groups ('PPS+' and 'PPS-').

Table S1. GEE results table with **static compliance** as the dependent variable, showing the values of the coefficients, the standard error, the value of Wald's χ^2 statistics, and p-value.

	Coefficients	Standard error	Wald's χ^2	p-value
Submerged GEE results, using the 'Intact' treatment as reference and an inverse link function				
Intercept	0.08	0.01	40.60	< 0.001
Submerged	-0.01	0.003	8.10	< 0.05
Post-pulmonary septum GEE results, using the 'Intact' treatment as reference and an inverse link function				
Intercept	0.08	0.01	41.40	< 0.001
PPS-	-0.05	0.01	27.20	< 0.001
PPS+	-0.05	0.01	32.90	< 0.001
Post-pulmonary septum GEE results, using the 'PPS+' treatment as reference and an inverse link				
Intercept	0.02	0.003	55.21	< 0.001
Intact	0.05	0.01	32.91	< 0.001
PPS-	0.000	0.001	0.01	0.94

Table S2. GEE results table for **dynamic compliance (C_{dyn})** and **work per ventilation (W)**, showing the degrees of freedom, the value of Wald's χ^2 statistics, and the p-value of each independent variable.

		DF	Wald's χ^2	p-value
Dynamic compliance				
Submerged				
	Treatment	1	6.00	0.01
	Volume	4	356.00	< 0.001
	Frequency	5	53.00	< 0.001
Post-pulmonary septum				
	Treatment	2	13.30	0.001
	Volume	4	42.20	< 0.001
	Frequency	5	41.60	< 0.001
Work per ventilation				
Submerged				
	Treatment	1	23.30	< 0.001
	Volume	4	49.60	< 0.001
	Frequency	5	11.80	0.03
Post-pulmonary septum				
	Treatment	2	8.90	0.01
	Volume	4	71.70	< 0.001
	Frequency	5	171.90	< 0.001

Table S3. GEE results table for **dynamic compliance (C_{dyn})**, showing the coefficients, the standard error, the value of Wald's χ^2 statistics, and p-value.

	Coefficients	Standard error	Wald's χ^2	p-value
Submerged GEE results, using the 'Intact' treatment, the "1 mL" volume, and the "05 min^{-1}" frequency as references				
Intercept	0.09	0.02	13.60	< 0.001
Submerged	0.01	0.009	4.32	0.03
2 ml	-0.02	0.004	29.05	< 0.001
4 ml	-0.04	0.01	20.03	< 0.001
6 ml	-0.04	0.01	11.57	< 0.001
8 ml	-0.03	0.01	7.67	< 0.001
10 min^{-1}	-0.001	0.001	0.80	0.37
20 min^{-1}	0.01	0.005	6.44	< 0.05
30 min^{-1}	0.02	0.009	5.25	< 0.05
40 min^{-1}	0.04	0.01	10.79	< 0.05
50 min^{-1}	0.05	0.01	9.75	< 0.05
Post-pulmonary septum GEE results, adopting an inverse link function and the 'Intact' treatment, the "1 mL" volume, and the "05 min^{-1}" frequency as references				
Intercept	0.03	0.01	7.72	0.005
PPS-	-0.02	0.009	7.43	0.006
PPS+	-0.03	0.01	8.89	0.002
2 ml	0.002	0.0005	15.74	< 0.001
4 ml	0.01	0.002	27.14	< 0.001
6 ml	0.02	0.004	21.25	< 0.001
8 ml	0.03	0.006	32.58	< 0.001
10 min^{-1}	0.002	0.002	1.24	0.26
20 min^{-1}	0.008	0.007	1.23	0.26
30 min^{-1}	0.02	0.01	3.55	0.05
40 min^{-1}	0.04	0.01	4.87	< 0.05
50 min^{-1}	0.05	0.02	5.86	< 0.05
Post-pulmonary septum GEE results, adopting an inverse link function and the "PPS+" treatment, the "1 mL" volume, and the "05 min^{-1}" frequency as references				
Intercept	0.009	0.004	3.63	< 0.001
Intact	0.03	0.01	8.90	< 0.001
PPS-	0.005	0.001	11.08	< 0.001
2 ml	0.002	0.0005	15.74	< 0.001
4 ml	0.01	0.002	27.14	< 0.001
6 ml	0.02	0.004	21.25	< 0.001
8 ml	0.03	0.006	32.58	< 0.001
10 min^{-1}	0.002	0.002	1.24	0.26
20 min^{-1}	0.008	0.007	1.23	0.26
30 min^{-1}	0.02	0.01	3.55	0.05
40 min^{-1}	0.04	0.01	4.87	< 0.05
50 min^{-1}	0.05	0.02	5.86	< 0.05

Table S4. GEE results table for **work per ventilation (W)**, showing the coefficients, the standard error, the value of Wald's χ^2 statistics, and p-values.

	Coefficients	Standard error	Wald's χ^2	p-value
Submerged GEE results, using the 'Intact' treatment, the "1 mL" volume, and the "05 min^{-1}" frequency as references				
Intercept	0.01	0.01	3.64	0.05
Submerged	0.0002	0.0008	0.04	0.83
2 ml	-0.0029	0.0029	0.98	0.32
4 ml	-0.01	0.01	1.87	0.17
6 ml	-0.01	0.01	2.68	0.1
8 ml	-0.01	0.01	2.85	0.09
10 min^{-1}	-0.0001	0.0002	0.66	0.42
20 min^{-1}	-0.0003	0.0001	4.99	< 0.05
30 min^{-1}	-0.0001	0.0003	0.03	0.86
40 min^{-1}	-0.0001	0.0005	0.04	0.85
50 min^{-1}	-0.0004	0.0007	0.42	0.52
Post-pulmonary septum GEE results, adopting an inverse link function and the 'Intact' treatment, the "1 mL" volume, and the "05 min^{-1}" frequency as references				
Intercept	0.096	0.03	10.32	0.001
PPS-	0.0004	0.0004	0.91	0.34
PPS+	0.0009	0.0009	1.09	0.30
2 ml	-0.05	0.02	10.14	0.001
4 ml	-0.08	0.03	9.12	< 0.005
6 ml	-0.08	0.03	9.08	< 0.005
8 ml	-0.09	0.03	9.39	< 0.005
10 min^{-1}	-0.003	0.001	22.35	< 0.001
20 min^{-1}	-0.005	0.001	23.51	< 0.001
30 min^{-1}	-0.01	0.001	33.06	< 0.001
40 min^{-1}	-0.01	0.001	30.28	< 0.001
50 min^{-1}	-0.01	0.002	30.2	< 0.001
Post-pulmonary septum GEE results, adopting an inverse link function and the "PPS+" treatment, the "1 mL" volume, and the "05 min^{-1}" frequency as references				
Intercept	0.09	0.03	11.07	< 0.001
Intact	-0.001	0.001	1.09	0.29
PPS-	-0.0005	0.001	0.35	0.55
2 ml	-0.05	0.02	10.14	0.001
4 ml	-0.08	0.03	9.12	< 0.005
6 ml	-0.08	0.03	9.08	< 0.005
8 ml	-0.09	0.03	9.39	< 0.005
10 min^{-1}	-0.003	0.001	22.35	< 0.001
20 min^{-1}	-0.005	0.001	23.51	< 0.001
30 min^{-1}	-0.01	0.001	33.06	< 0.001
40 min^{-1}	-0.01	0.001	30.28	< 0.001
50 min^{-1}	-0.01	0.002	30.2	< 0.001